IOP Publishing Quantum Sci. Technol. 8 (2023) 025007 https://doi.org/10.1088/2058-9565/acb4b8

Quantum Science and Technology

OPEN ACCESS

RECEIVED
25 August 2022

REVISED
9 December 2022

ACCEPTED FOR PUBLICATION
19 January 2023

PUBLISHED
2 February 2023

PAPER

A multiplexed synthesizer for non-Gaussian photonic quantum state generation

M F Melalkia[1], J Huynh[1], S Tanzilli[1], V D'Auria[1,2] and J Etesse[1,*]

[1] Université Côte d'Azur, CNRS, Institut de Physique de Nice (INPHYNI), UMR 7010, Parc Valrose, Nice Cedex 2, France
[2] Institut Universitaire de France (IUF), France
* Author to whom any correspondence should be addressed.

E-mail: jean.etesse@inphyni.cnrs.fr

Keywords: quantum optics, non-Gaussian states, continuous variables, Schrödinger cat states, GKP states

Supplementary material for this article is available online

Abstract

Disposing of simple and efficient sources for photonic states with non-classical photon statistics is of paramount importance for implementing quantum computation and communication protocols. In this work, we propose an innovative approach that drastically simplifies the preparation of non-Gaussian states as compared to previous proposals, by taking advantage from the multiplexing capabilities offered by modern quantum photonics tools. Our proposal is inspired by iterative protocols, where multiple resources are combined one after the other for obtaining high-amplitude complex output states. Here, conversely, a large part of the protocol is performed in parallel, by using a single projective measurement along a mode which partially overlaps with all the input modes. We show that our protocol can be used to generate high-quality and high-amplitude Schrödinger cat states as well as more complex states such as error-correcting codes. Remarkably, our proposal can be implemented with experimentally available resources, highlighting its straightforward feasibility.

1. Introduction

Efficient coding of quantum information relies on the capability to generate high-quality states of light with non-classical photon statistics, both in the continuous- [1] and discrete-variable [2] regimes. In particular, states with negative Wigner functions have shown to be crucial for implementing sophisticated protocols and information processing [3, 4], such as error-correction [5] and one-way quantum computing [6]. Different strategies for generating such states were reported, relying for instance on high-order nonlinearity [7–9], qubit interaction [10] and linear optical interaction with non-Gaussian resources such as Fock states or photon counting [11–15]. A class of protocols of particular interest is that of iterative schemes [11–13, 15–17], where photonic 'resource' states are combined together in an iterative fashion, allowing for growing step-by-step the size of the states. However, the experimentally implemented protocols are to date restricted to few operations, due to protocol scalability issues arising from the simultaneous need for multiple heralding signals and from the increase of experimental overhead [18, 19]. This ultimately limits the average photon number in the generated state.

In this article, we propose a novel scheme to overcome the current experimental limitations, by relying on a single shot operation with a spectrally multiplexed resource. Our proposal takes advantage of the multimode aspect of state-of-the-art experimentally investigated quantum photonic sources in order to greatly enhance the capabilities of iterative generation protocols. This improvement occurs at two levels: (a) the number of operations to implement is reduced to one, and, as a consequence, (b) the success probability of the overall operation is strongly increased. To illustrate our proposal, we show that Schrödinger cat state (SCS) and GKP-codes [5] can be generated in an efficient manner, proving the validity of the approach, and opening a new path in the domain of non-Gaussian photonic state preparation.

In section 2 we recall the principle of iterative protocols and propose a fully parallelized counterpart relying on spectral multimode quantum optics. Section 3 is devoted to the investigation of parallelized generation of cat states and GKP codes. Finally, in section 4, we show that our protocol can be used with experimental readily accessible resources such as single photon Fock states.

2. Multimode iterative protocol

2.1. Framework: iterative protocols

The protocol proposed in this paper takes its essence from iterative generation protocols, an elementary brick of which is represented in figure 1.

Such operation consists in mixing two input 'resource' states, $|\psi_0\rangle$ and $|\psi_1\rangle$, on a beamsplitter with transmittivity τ_0, to herald the generation of an output state $|\psi_{\text{out}}\rangle$. The heralding process can be performed in different ways [12, 15], and even if the results derived here can easily be extended to the photon counting case, we focus in the following on homodyne conditioning. The main difference in these two approaches is that in the photon counting case one can rely on Gaussian input states while requiring photon counting devices [14, 15], whereas in the homodyne conditioning case, Gaussian transformations and heralding are sufficient while requiring non-Gaussian input resource states [12, 13]. In this scenario, one of the two output arms of the beamsplitter is measured by a homodyne detector (along a certain quadrature x_θ). When the measurement outcome is close enough to an assigned value ($x_\theta = x_0$ on figure 1), the target output state is successfully heralded. The strength of such a protocol is that the average photon number of the output state can be higher than the one of each individual input states. Accordingly, it can be used to 'breed' complex photonic states by cascading the protocol using $|\psi_{\text{out}}\rangle$ as one of the input of a subsequent operation.

Figure 2 shows such a configuration, where states of increasing size are combined with resource states; tree-like configurations are also commonly investigated, thanks to the parallelization capabilities they offer [17]. This idea is at the core of the 'cat breeding' scheme, proposed in [11], where balanced beamsplitter ($\tau = 1/\sqrt{2}$) and $x_i = 0$ homodyne conditioning are used [20, 21]. In this case, mixing two SCSs allows to create a single SCS with an amplitude increased by a factor $\sqrt{2}$. Iterating this protocol N times then allows to create a SCS with an amplitude amplified by a factor $2^{N/2}$. An alternative manner has also been proposed, where the input cat states were replaced by single photons, allowing the production of squeezed SCSs, robuster to losses [12, 22]. We note that the increase of the amplitude of the output state is closely related to the 'Wigner negativity concentration' phenomenon, as treated in [23]. By modifying the quadrature along which the homodyne conditioning is performed ($p = 0$ homodyne conditionings), GKP codes can be generated all-optically [17, 24]. More generally, all superpositions of up to N photons can be generated by properly adjusting the beamsplitter reflectivities and homodyne conditionings [12].

Proof-of principle experimental validations are currently limited to single stage implementations due to scalability issues [18, 19]: in bulk optics, increasing the number of stages by increasing the number of input state sources indeed leads to intractable complexities. Temporal multiplexing represents a promising alternative that is also investigated [25], but could ultimately lead to a decrease in the overall generation rate of the states. Integrated optics, on the other hand, offers an attractive solution to address spatial scalability issues, but inevitable losses associated with such platforms should be carefully taken into consideration [26].

We propose in this article to rely instead on spectral multiplexing, which offers an increased generation efficiency as well as noticeable experimental simplifications.

2.2. Multiplexed single-stage generation protocol

The main idea of the proposal, sketched in figure 3, consists in the following key ingredients. To begin with, a 'seed' state $|\psi_0\rangle$ initially populates a spectral mode $\chi_0(\omega)$ in which the quantum engineering process is to be performed. In output of the protocol, we will focus on the state ρ_{out} that populates this same mode $\chi_0(\omega)$. Subsequently, we select a collection of states $|\psi_0'\rangle, |\psi_1'\rangle, \ldots, |\psi_{N-2}'\rangle$ respectively in modes $\varphi_0(\omega)$, $\varphi_1(\omega), \ldots, \varphi_{N-2}(\omega)$ that are used to 'feed' the protocol, so as to grow the overall size of the output state ρ_{out}. As will be discussed with a concrete example, the spectral modes $\varphi_i(\omega)$ have to overlap $\chi_0(\omega)$ in a clever way, so that each $|\psi_i'\rangle$ contributes in an efficient manner to the generation protocol. This collection of states is merged in a single spatial mode and sent to the first input port (port a) of a beamsplitter of transmittivity τ so as to interfere with the seed state $|\psi_0\rangle$ sent to the other input port of this beamsplitter (port b). Importantly, a perfect spatial mode matching of the two states populating modes a and b must be guaranteed. After interaction, one output port of the beamsplitter is measured by a homodyne detector along mode $\chi_0(\omega)$, to perform the desired conditioning $x_\theta = x_0$, for successfully heralding the generation of a state ρ_{out} on the other output port.

A major advantage of this method is that it allows mixing N states in a single heralding step, therefore drastically increasing the success probability of the protocol and reducing the experimental complexity as

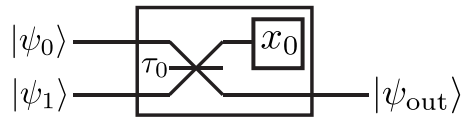

Figure 1. Elementary brick of an iterative protocol.

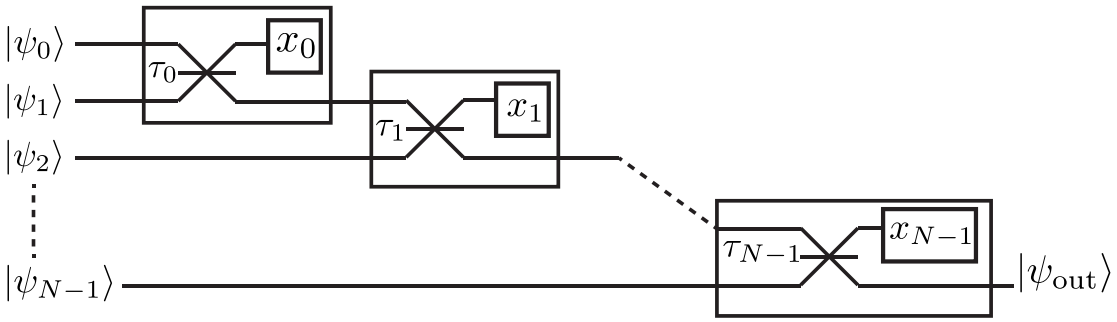

Figure 2. A cascaded architecture for an iterative protocol.

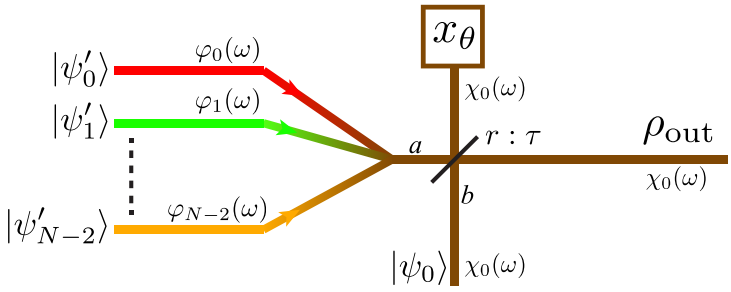

Figure 3. The multiplexed generation protocol (see text for description).

compared with the standard spatial multiplexing strategy, as will be quantitatively shown later. Moreover, iterative protocols usually require a fixed phase relationship between each arms, implying interferometric stability in experimental implementations, which can be quickly limiting in terms of complexity. Here, as we beneficiate from other degrees of freedom than the spatial one, this interferometric stability is inherently guaranteed, strongly simplifying the setups.

It shall be noticed at this point that in contrast with the iterative protocol of figure 2, the merging of the spectral modes must be accompanied with losses, whose influence strongly depend on the resource states. This will be detailed in section 3.

The multimode description that we use complies with realistic implementations of Gaussian state sources, such as, for instance, multimode squeezed vacuum sources [27]. It is now indeed well established that spontaneous parametric down-conversion (SPDC) through three-wave mixing process produces a collection of squeezed vacuum states in separate orthogonal spectral modes $\{\varphi_k(\omega)\}_{k\in\mathbb{N}}$, each with a different squeezing parameter [28, 29].

More generally, each spectral mode $\varphi_k(\omega)$ can be associated with a bosonic annihilation operator $\hat{A}_k$:

$$\hat{A}_k = \int \varphi_k^*(\omega)\hat{a}(\omega)d\omega, \tag{1}$$

$\{a(\omega)\}$ being the bosonic operators of individual spectral components at the SPDC output. When two different sets of modes $\{\varphi_k(\omega)\}_{k\in\mathbb{N}}$ and $\{\chi_l(\omega)\}_{l\in\mathbb{N}}$ are involved, one can express their 'likeness' by using the overlap formula:

$$c_{k,l} = \int \varphi_k^*(\omega)\chi_l(\omega)d\omega. \tag{2}$$

This formula allows switching from one mode basis to the other thanks to:

$$\varphi_k(\omega) = \sum_l c^*_{k,l}\chi_l(\omega). \tag{3}$$

We show in the next paragraph that the proposed protocol can be used to generate highly-fidel SCSs and GKP codes with increased success probabilities compared to standard iterative protocols.

3. Paralellized generation of complex photonic states

3.1. Parallel cat 'breeding'

The previously described scheme can be applied to the generation of large amplitude SCSs, inspired by cat 'breeding' iterative protocols. To perform such a generation, we simply consider here $N \geqslant 2$ identical SCS input states of amplitude α in the $N-1$ input modes $\varphi_k(\omega)$:

$$\forall k, \in [\![0, N-2]\!],\ |\psi'_k\rangle = |\psi_0\rangle = \frac{1}{\mathcal{N}}\left(|\alpha\rangle + |-\alpha\rangle\right), \tag{4}$$

where $\mathcal{N} = \sqrt{2\left(1+e^{-2|\alpha|^2}\right)}$ is a normalization factor. Note that we restrict the discussion to even cat states, but similar reasoning is also valid with odd cat states, as treated in the supplementary material. Then we set that each mode $\varphi_k(\omega)$ is of equal contribution in the generation process, namely $\forall k \in [\![0, N-2]\!]$:

$$c_{k,0} = \int \varphi^*_k(\omega)\chi_0(\omega)d\omega = \frac{1}{\sqrt{N-1}}. \tag{5}$$

In this way, each input 'feeding' cat $|\psi'_k\rangle$ will 'breed' the input seed cat $|\psi_0\rangle$ by the same amount. Subsequently, homodyne conditioning is performed along the x quadrature (in-phase with the SCS) around $x=0$, within a given acceptance window $[-\Delta x/2, \Delta x/2]$. An analytic formula for the output Wigner function (see supplementary material) can then be derived, allowing us to predict the performances of the protocol as a function of key parameters such as r, N, α and the heralding width Δx. Many different metrics can be used to quantify the distance between an output state and a target state. Here, the fidelity of ρ_{out} with the nearest ideal SCS is used (amplitude γ). In order to assess the performances of the protocol in terms of state synthesis and optimal generation parameter choices, we consider the case of an infinitely thin heralding window here $\Delta x \to 0$, with the exception of figure 6, where the success probability of the protocol is estimated. The dependence of the fidelity with the heralding window Δx is studied in the supplementary material IV.B, and reveals that high fidelity can be reached together with high success probability.

3.1.1. Beamsplitter reflectivity

The aforementioned fidelity of the output state is plotted in figures 4(a)–(d) for $N = 2$, 3, 6 and 8 input SCSs of amplitude $\alpha = 3$, as a function of the beamsplitter reflectivity τ and of the output state amplitude γ. These plots clearly reveal that the output amplitude of the cat state in mode $\chi_0(\omega)$ that corresponds to optimal fidelities with ρ_{out} grows with the number of input states. This successfully proves the breeding of the input SCSs. Figure 4 also shows that the reflectivity should be optimized in a non-trivial way, according to the number of input breeding states, in order to maximize the output state fidelity with high-amplitude SCSs.

To gain a qualitative intuition on the quality of the multimode breeding operation, the Wigner functions of the corresponding output states are plotted in figures 4(e)–(h), showing their strong non-classical signature, as the Wigner functions contain oscillations with negative values. To be more quantitative on this result, the numerical values of fidelity, optimal reflectivity and output SCS amplitudes are also written on figures 4(a)–(d), revealing the very high fidelities of the output states with high-amplitude SCSs. In addition, it confirms that the amplitude of the output SCS increases with N, with a scaling of the order of $\gamma \sim \sqrt{N}\alpha$.

3.1.2. Amplitude of the input states

The protocol is also sensitive to the amplitude of the input cat states. This is illustrated in figure 5, where the output state fidelity $\mathcal{F}$ with the nearest cat state is represented as a function of the input SCS amplitude α, for different numbers of input states N. Two important trends shall be noticed: (a) for a given α, increasing N decreases the overall output state fidelity. However, (b) increasing α for a given N leads to an increased global fidelity. For instance, to create states with 99% fidelity with $N = 2$, an input amplitude $\alpha = 1.13$ is sufficient, whereas $\alpha = 2.49$ is required to reach the same fidelity with $N = 4$ input states. In the case of even cat states that are considered here, there is also an increase of the fidelity for vanishing α simply because vacuum is a perfect even cat state with zero amplitude, a case of no interest for us.

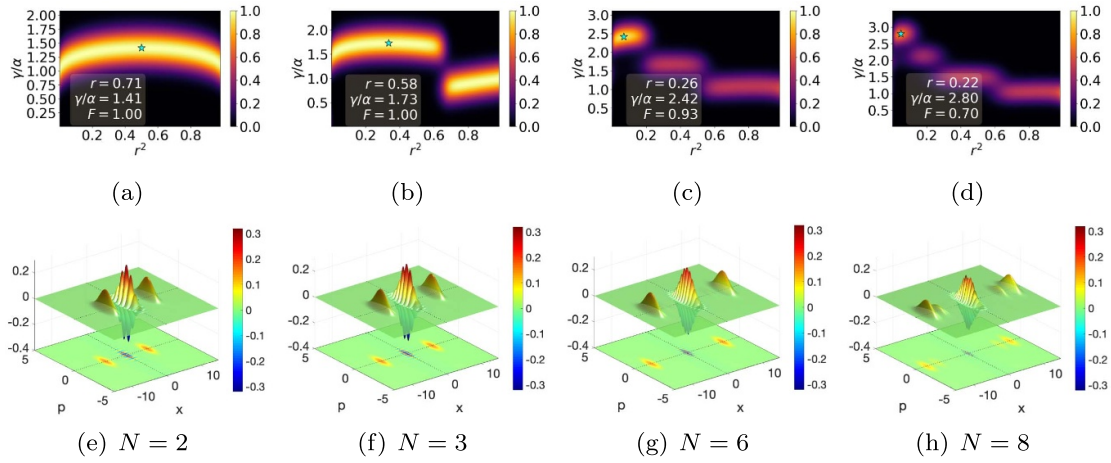

Figure 4. Fidelity $\mathcal{F}$ of the output state with a cat state of amplitude γ as a function of the beamsplitter reflectivity r, for (a) $N=2$, (b) $N=3$, (c) $N=6$ and (d) $N=8$ input cat states of amplitude $\alpha=3$. In each plot, a star spots the highest fidelity point, and the corresponding parameters are given in the insets. The Wigner functions corresponding to this maximal fidelity point are represented in (e)–(h) respectively.

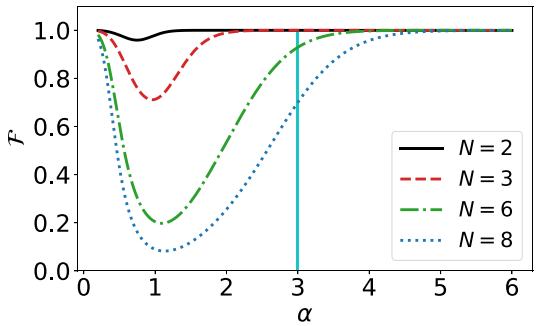

Figure 5. Fidelity of the output state with the nearest SCS as a function of the input SCS amplitude α, for different N. The cases represented in figure 4 correspond to the vertical blue line ($\alpha=3$).

3.1.3. Comparison with the iterative cat breeding protocol

Interestingly, we can draw a direct parallel with the iterative cat breeding protocol, where $N-1$ heralding steps are performed on N input resources. The main difference, however, is that the multimode protocol that we propose here is inevitably accompanied with information loss due to partial overlap of the spectral modes $\varphi_k(\omega)$ with the output mode of interest $\chi_0(\omega)$. Equation (5) directly shows that each mode $\varphi_i(\omega)$ overlaps only partially with $\chi_0(\omega)$, therefore all of the components of the input states $|\psi_i'\rangle$ along $\chi_{l>0}(\omega)$ are purely lost during the process, where $\{\chi_l(\omega)\}_{l\in\mathbb{N}}$ constitutes a complete spectral basis. Therefore, the output state ρ_{out} cannot be a pure state as long as more than two modes are populated in total.

To give an intuitive model, we propose a simple parallel between spatial and spectral modes: the operation depicted in figure 3 by the merging arrows from modes $\varphi_k(\omega)$ to $\chi_0(\omega)$ can actually be simply modelled as a $N-1$ input/$N-1$ output beamsplitter transformation, where $N-2$ outputs are lost in the environment. This transformation is exactly the one depicted in figure 2 for input states $|\psi_0\rangle$ to $|\psi_{N-2}\rangle$, with $\tau_i=\sqrt{(i+1)/(i+2)}$ so as to obtain $c_{0,k}=1/\sqrt{N-1}$. In other words, our protocol is equivalent to the iterative breeding scheme of figure 2, where only the last heralding step $x=x_{N-1}$ is performed and all the other ones are simply ignored. The direct consequence for this is that the overall success probability of the protocol is increased by several orders of magnitude as compared to the iterative scheme. This is illustrated in figure 6, where the success probability of our scheme for input SCS amplitudes of $\alpha=3$ and $N=4$ is plotted, in comparison with the iterative scheme of figure 2 in the case where all the heralding widths are identical. The cost obviously is the overall fidelity, which is degraded in the multimode case, but nevertheless remains very high, as we have seen in figure 4. The multimode protocol therefore takes advantage of the robustness of the breeding protocol for imperfect heralding at sufficiently high SCS amplitudes.

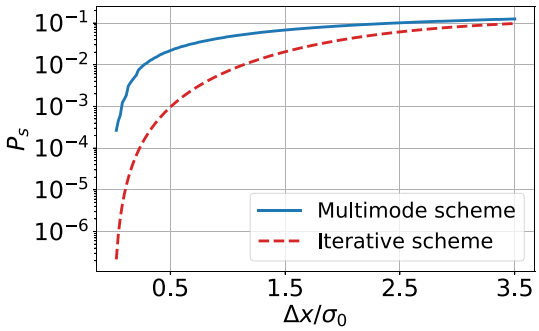

Figure 6. Comparison between the success probability P_S of the multimode scheme and the iterative scheme for $N = 4$, as a function of the heralding window Δx normalized to the shot noise standard deviation σ_0.

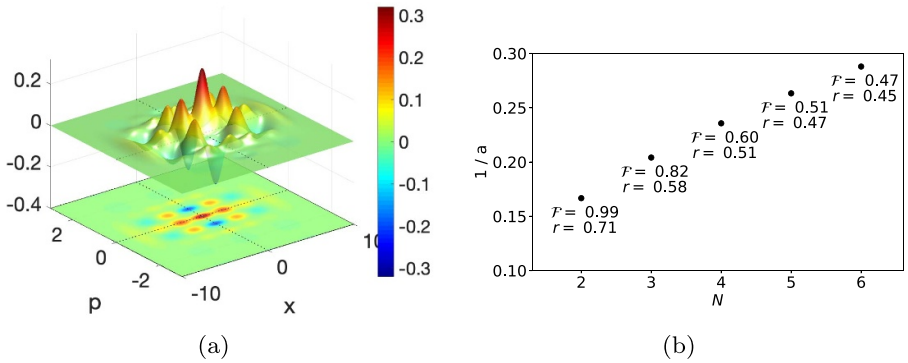

Figure 7. Performance of the multiplexed protocol for the generation of approximate GKP codes. (a) Wigner function of the output state with $N = 3$ input SCSs of amplitude $\alpha = 3$. (b) GKP state amplitude $1/a$ (see equation (6)) when the number of input cat states N is increased. The fidelity $\mathcal{F}$ with the closest perfect GKP state is given for each point, with the corresponding beamsplitter reflectivity r.

3.2. GKP states preparation

In addition to the generation of SCSs, our protocol can also advantageously be applied to for the generation of more complex states such as the GKP codes [5]. These states were first introduced as a means to encode information in an oscillator, with an error-correcting capability. They were recently generated and used in trapped ions [30] and superconducting circuits [31], but still remain out of reach of all-optical protocols. Here, we can use the same protocol as the one depicted in section 3.1 ($N-1$ input cat states in modes φ_k and one cat state in mode χ_0, all of amplitude α), with the only difference that homodyne conditioning is performed along $x_{\pi/2} := p = 0$. Such conditioning has already been investigated in the context of all-optical generation of GKP with iterative protocol [17, 24]. We show here that it can be transposed to our multiplexed approach. As a reminder, the wavefunctions of approximate GKP codes $|\tilde{0}\rangle$ and $|\tilde{1}\rangle$ take the form:

$$\langle x|\tilde{0}\rangle = \frac{1}{\mathcal{N}_0}\sum_{k\in\mathbb{Z}} e^{-\frac{s_1^2}{2}(ka)^2} e^{-\frac{1}{2s_2^2}(x-ka)^2}, \tag{6a}$$

$$\langle x|\tilde{1}\rangle = \frac{1}{\mathcal{N}_0}\sum_{k\in\mathbb{Z}} e^{-\frac{s_1^2}{2}(k+1/2)^2a^2} e^{-\frac{1}{2s_2^2}(x-(k+1/2)a)^2}, \tag{6b}$$

where $1/s_1$ gives the overall envelope size of the state, s_2 is the standard deviation of each tooth in the distribution, and a is the distance between consecutive teeth along the x quadrature. Figure 7(a) shows the shape of the Wigner function of the output state for $N = 3$, revealing the grid structure specific to GKP codes. Such likeness is, here again, quantified by the fidelity with the nearest GKP code, that we plot in figure 7(b). This figure shows that augmenting the amount of input resources indeed increases the size of the output state along the opposite quadrature ($1/a$), while requiring an optimization of r. Similarly to the SCS case, it also shows that the fidelity decreases with N.

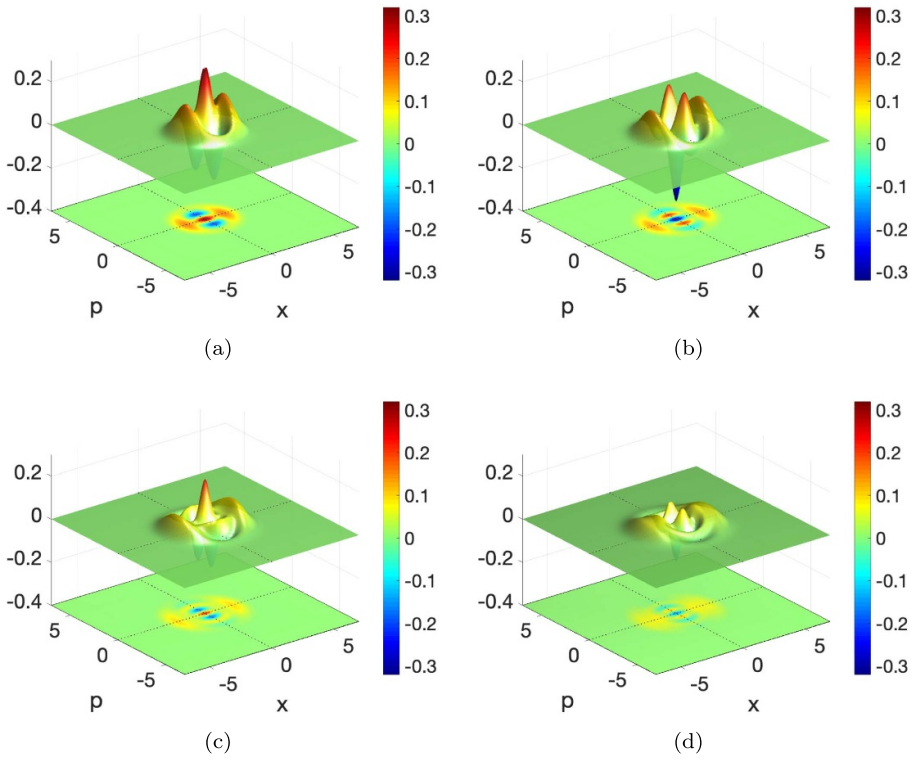

Figure 8. Wigner functions of the output state of the protocol fed by single photon Fock states, with (a) $N = 2$, (b) $N = 3$, (c) $N = 4$ and (d) $N = 5$.

4. Proposal with experimentally accessible resources

An important aspect of our strategy is that it can directly be implemented with already accessible experimental resources. Even if high-amplitude SCSs are not trivial to generate experimentally, good approximation of them at low amplitudes (also called Schrödinger 'kitten' states) are commonly produced states. Moreover, the breeding principle has been experimentally demonstrated with kittens, showing the validity of the approach [19]. In addition, single photon Fock states also constitute a valid alternative to them, as theoretically and experimentally demonstrated [17, 18], to generate squeezed SCS-like output states with high fidelity. It is worth noting that squeezing the output states constitutes a high advantage, as it can increase their robustness to losses [22, 32]. Accordingly, the results presented here will focus on input single photon Fock states. Very similar results are expected with kitten states.

4.1. Generation with multiplexed single photons

We recall that our protocol requires the use of a multiplexed input state source. This can simply be achieved by taking advantage of the spectral tailoring possibility that processes like spontaneous parametric down-conversion offer [28]. Indeed, depending on the pumping and phase-matching conditions, two-mode squeezing can be generated along a large number of spectral modes, offering the ideal platform for multiplexed generation [29]. Then, single photon Fock states are simply heralded by performing a projective measurement over one of the two mode squeezing subsystems. This method, although very commonly used for the generation of high-quality single photon Fock states for a couple of decades now, has recently been extended experimentally to high-dimension mode-selective quantum state tailoring [33, 34]. This allows to tweak the supermode in which the single photon detection occurs, therefore heralding a single photon Fock state in a given supermode. Here we can take advantage of such capabilities, by using multiplexed photon sources to feed the protocol and generate complex photonic states in a single shot.

The output Wigner functions of the protocol fed by an increasing number N of single photon Fock states are shown in figure 8. They clearly reveal that the output state contains more and more oscillations at its centre with increasing N. To be more quantitative, table 1 gathers the parameters of the closest SCS, where α is the amplitude, s its compression parameter and $\mathcal{F}$ the fidelity between the two states. This table reveals that the amplitude of the state increases with N for low values, but degrades after $N = 4$. Further simulations

Table 1. Fidelity of the output state with a squeezed SCS of amplitude α and squeezing s.

	$N=2$	$N=3$	$N=4$	$N=5$	$N=6$
α	1.63	2.03	2.30	2.12	1.78
s	0.66	0.65	0.66	0.74	0.75
$\mathcal{F}$	0.99	0.90	0.66	0.49	0.37

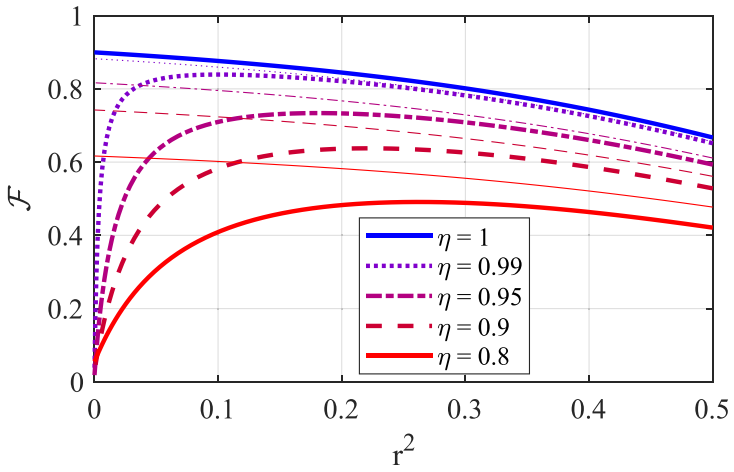

Figure 9. Dependency of the output state fidelity $\mathcal{F}$ with a squeezed SCS of amplitude $\alpha = 2.03$ and squeezing factor $s = 0.65$ as a function of the beamsplitter reflectivity r^2, for $N = 3$, for different values of η. As a comparison, thin lines with equivalent symbols correspond to perfect input single photons, and an output state which has endured losses of transmission η.

show that this is true for larger N as well. Such an evolution can qualitatively be explained by the phase invariance of the two states impinging the beamsplitter: as the only rotation symmetry breaking operation is the homodyne measurement, the fidelity of the created state with a highly non-phase invariant state decreases with its size.

It should also be pointed that the optimal generation condition (highest amplitude and fidelity) is fulfilled with the use of a beamsplitter with vanishing reflectivity. This is shown in figure 9, in the solid blue line (case $\eta = 1$, see study below for notations).

4.2. Effect of imperfections

Our analysis reveals that few-mode single photon states are relevant resources for our protocol in order to produce high-quality SCSs, essential brick in continuous-variable quantum information processing. In practice, perfectly pure single photons are not available, and imperfections must usually be taken into account. Though it is not the scope of this paper to encompass the whole variety of such imperfections, we can give a glimpse on the effect of a common one. If we consider that each input resource state is of the form:

$$\rho_{\text{in}} = \eta|1\rangle\langle 1| + (1-\eta)|0\rangle\langle 0|, \tag{7}$$

we can emulate the impurity of photons. Namely, this takes into account losses of transmission η endured by the photons. Note that in our multiplexed scheme, this is mathematically equivalent to disposing of perfect input photons, and to applying losses of transmission η in both output arms of the mixing beamsplitter. This in turn has two effects. The first (I) is on the homodyne heralding: adding losses in the heralding path is equivalent to disposing of inefficient homodyne detection for the heralding. We derive in supplementary material Section IV the effect of such loss, and find that they are equivalent to widening the heralding window by a factor $\sqrt{(1-\eta)/2}$ while making it more and more Gaussian. The second effect of losses (II) turns to applying a transmission η to the output state. Obviously, the larger the output SCS, the more sensitive to losses it will be. Fortunately, as stated before, the squeezed SCSs generated by this protocol are more robust to losses, compared to SCSs [22, 32], so we expect a higher resilience to input state imperfections. We plot in figure 9 the fidelity of the output state with a squeezed SCS of amplitude $\alpha = 2.03$ and squeezing factor $s = 0.65$ for $N = 3$ input single photons (expected parameters, see table 1), for different values of η (thick lines). A striking fact is that for a given η, the maximal fidelity is reached for an optimal reflectivity that depends on η. In particular, as soon as imperfections are introduced in the input state, a

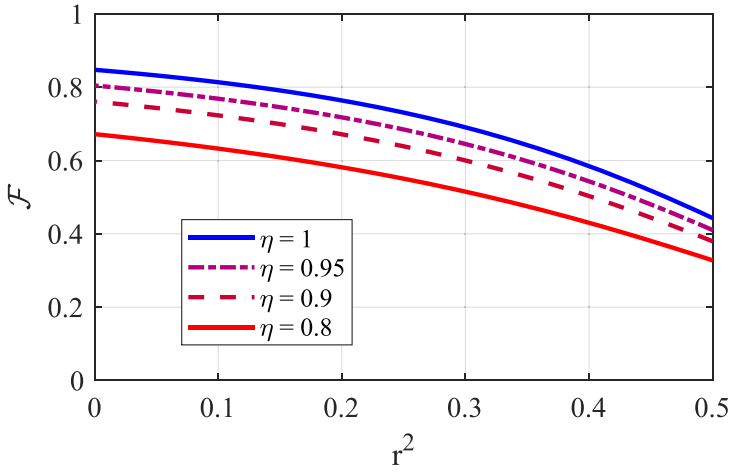

Figure 10. Fidelity of the output of the protocol with a SCS with parameters $\alpha = 2.25$ and $s = 0.67$, for $N = 3$ and $x = 0$ heralding. Here, the resource state is the outcome of the multiplexed protocol with two resource states (7) of various η parameters, $x = 0$ heralding and $r^2 = 1/2$.

vanishing reflectivity yields a very low fidelity state (see the drop in fidelity close to $r^2 = 0$ between $\eta = 1$ and $\eta = 0.99$ on figure 9). This can simply be explained by the fact that if the reflectivity is small enough, the state reaching the homodyne detection used to herald the state is actually close to $|\psi_0\rangle$. If any imperfection is added to the state, heralding on $x \simeq 0$ is mainly triggered by the vacuum contribution in this state, and not by the fraction of the state reflected by the beamsplitter. A different way of interpreting this is to come back to the two effects (I) and (II) of losses we introduced before: the sole effect of losses on the output state (II) are shown figure 9 with thin lines (equivalent line symbols and colors for various η). For low values of r^2, these curves clearly diverge from the actual ones, revealing that in this regime the dominant effect of the imperfections is (I), the effective broadening of homodyne heralding by a factor of $\sqrt{(1-\eta)/2}$.

4.3. Discussion

According to our previous study, in order to generate highly fidel output state, we have two main strategies at our disposal. The most straightforward consists in increasing the quality of the resource states, in order to bring η as close to 1 as possible. However, in practice experimental limitations often preclude increasing the fidelity of the state to arbitrarily high values. Moreover, as we have seen with the effect of part (I) of the imperfections, even if η is arbitrarily close to 1, aiming at a vanishing reflectivity r^2 imposes to narrow the heralding width Δx accordingly, therefore reducing the heralding rate.

Luckily, a different strategy is possible, which consists in mixing the usual iterative schemes with our multiplexed picture. Indeed, it should be stressed that when the amplitude of the SCSs that feed the protocol is increased, the sensitivity of the protocol to the heralding width window Δx is decreased. In section IV of supplementary material, we indeed show that increasing the heralding width Δx from 0 to σ_0 does not drastically decrease the output state fidelity when the resource states are SCSs of amplitude $\alpha = 3$. This means that if we combine the usual approach of iterative schemes with our multiplexed proposal, we could in principle optimize the output state fidelity by adding additional heralding steps.

We illustrate this with a concrete example: in figure 10, we plot the fidelity of the output state with a SCS of amplitude $\alpha = 2.25$ and squeezing factor $s = 0.67$ for a protocol with $N = 3$ input resource states as a function of the beamsplitter reflectivity r^2. The particularity here is that the resource states is not (7) anymore, but it is the outcome of a $N = 2$ protocol with resource states (7) in input and a $r^2 = 0.5$ beamsplitter. Therefore, we have cascaded two multiplexed schemes, requiring three homodyne heralding in total. A fist striking fact here is that with this hybrid scheme, we pushed the fidelity of the scheme with a total of 6 input imperfect photons (two per resource state) from below 40% (see table 1) to more than 80%. Secondly, the sensitivity to losses is, as expected, much lower than in the case of figure 9, thanks to the larger amplitude of the resource states, as expected. Note also that in this hybrid approach, only 4 homodyne heraldings are required in total, whereas 5 should be used in the usual iterative scheme [12]. We believe that adapting the protocol architecture with respect to the input state imperfections and expected output quality is possible with our scheme, and that such optimization should be conducted systematically regarding to the specific conditions. Methods such as backcasting search could for instance help in this direction [35]. Such study however goes beyond the scope of this paper.

5. Conclusion

We have proposed and discussed an innovative protocol for the generation of non-Gaussian states of light. Our scheme is inspired by iterative protocols but takes advantage of multiplexing capabilities of photonics resources. It relies on the use of multiple states in a single spatial mode but multiplexed in an other degree of freedom, mixed with a resource state whose mode partially overlaps all input states. By performing a homodyne conditioning after mixing the states at a beamsplitter, complex output states can be produced. The major strength of our proposal is that no cascade manipulation steps are required for the state breeding, therefore strongly simplifying the experimental implementation in a one-shot scheme, and allowing to access high-success rates. We have shown that frequency multiplexing can be used for the generation of high-quality and high-amplitude Schrödinger cat and GKP states, by using as input states small-amplitude SCS, or alternatively, readily accessible experimental resources such as multiplexed single photon Fock states. Note that current state-of-the-art non-linear sources offer the capability for generating such states by providing the native generation of frequency multiplexed single- and two-mode squeezing. Due to its high efficiency and simplified implementation as well as to the possibility of implementing it with already available experimental resources, we believe that our approach to non-Gaussian state preparation represents an appealing alternative in the domain of non-classical photonic state generation, and will open a wide range of applications.

Data availability statement

The data that support the findings of this study are available upon reasonable request from the authors.

Acknowledgments

This work has been conducted within the framework of the project HyLight (No. ANR-17-CE30-0006-01) granted by the Agence Nationale de la Recherche (ANR). Virginia D'Auria acknowledges the Institut Universitaire de France (IUF).

ORCID iDs

M F Melalkia https://orcid.org/0000-0001-7694-9261
S Tanzilli https://orcid.org/0000-0003-4030-5821
J Etesse https://orcid.org/0000-0001-6616-5607

References

[1] Lvovsky A I, Grangier P, Ourjoumtsev A, Parigi V, Sasaki M and Tualle-Brouri R 2020 Production and applications of non-Gaussian quantum states of light (arXiv:2006.16985)
[2] Zhong H-S *et al* 2020 Quantum computational advantage using photons *Science* **370** 1460–3
[3] Mari A and Eisert J 2012 Positive Wigner functions render classical simulation of quantum computation efficient *Phys. Rev. Lett.* **109** 230503
[4] Veitch V, Ferrie C, Gross D and Emerson J 2012 Negative quasi-probability as a resource for quantum computation *New J. Phys.* **14** 113011
[5] Gottesman D, Kitaev A and Preskill J 2001 Encoding a qubit in an oscillator *Phys. Rev.* A **64** 012310
[6] Zheng Y, Hahn O, Stadler P, Holmvall P, Quijandría F, Ferraro A and Ferrini G 2021 Gaussian conversion protocols for cubic phase state generation *PRX Quantum* **2** 010327
[7] Hacker B, Welte S, Daiss S, Shaukat A, Ritter S, Li L and Rempe G 2019 Deterministic creation of entangled atom–light Schrödinger-cat states *Nat. Photon.* **13** 110–15
[8] Fukui K, Endo M, Asavanant W, Sakaguchi A, Yoshikawa J-ichi and Furusawa A 2022 Generating the Gottesman–Kitaev–Preskill qubit using a cross-Kerr interaction between squeezed light and Fock states in optics *Phys. Rev.* A **105** 022436
[9] Wang Z *et al* 2022 A flying Schrödinger's cat in multipartite entangled states *Sci. Adv.* **8** eabn1778
[10] Hastrup J, Park K, Brask J B, Filip R and Andersen U L 2021 Measurement-free preparation of grid states *npj Quantum Inf.* **7** 17
[11] Lund A P, Jeong H, Ralph T C and Kim M S 2004 Conditional production of superpositions of coherent states with inefficient photon detection *Phys. Rev.* A **70** 020101
[12] Etesse J, Kanseri B and Tualle-Brouri R 2014 Iterative tailoring of optical quantum states with homodyne measurements *Opt. Express* **22** 30357–67
[13] Weigand D J and Terhal B M 2018 Generating grid states from Schrödinger-cat states without postselection *Phys. Rev.* A **97** 022341
[14] Su D, Myers C R and Sabapathy K K 2019 Conversion of Gaussian states to non-Gaussian states using photon-number-resolving detectors *Phys. Rev.* A **100** 052301
[15] Eaton M, Nehra R and Pfister O 2019 Non-Gaussian and Gottesman–Kitaev–Preskill state preparation by photon catalysis *New J. Phys.* **21** 113034
[16] Fiurášek Jır, García-Patrón R and Cerf N J 2005 Conditional generation of arbitrary single-mode quantum states of light by repeated photon subtractions *Phys. Rev.* A **72** 033822
[17] Etesse J, Blandino R, Kanseri B and Tualle-Brouri R 2014 Proposal for a loophole-free violation of Bell's inequalities with a set of single photons and homodyne measurements *New J. Phys.* **16** 053001

[18] Etesse J, Bouillard M, Kanseri B and Tualle-Brouri R 2015 Experimental generation of squeezed cat states with an operation allowing iterative growth *Phys. Rev. Lett.* **114** 193602
[19] Sychev D V, Ulanov A E, Pushkina A A, Richards M W, Fedorov I A and Lvovsky A I 2017 Enlargement of optical Schrödinger's cat states *Nat. Photon.* **11** 379 E
[20] Takeoka M and Sasaki M 2007 Conditional generation of an arbitrary superposition of coherent states *Phys. Rev.* A **75** 064302
[21] Brask J B, Rigas I, Polzik E S, Andersen U L and Sørensen A S 2010 Hybrid long-distance entanglement distribution protocol *Phys. Rev. Lett.* **105** 160501
[22] Le Jeannic H, Cavaillès A, Huang K, Filip R and Laurat J 2018 Slowing quantum decoherence by squeezing in phase space *Phys. Rev. Lett.* **120** 073603
[23] Albarelli F, Genoni M G, Paris M G A and Ferraro A 2018 Resource theory of quantum non-Gaussianity and Wigner negativity *Phys. Rev.* A **98** 052350
[24] Vasconcelos H M, Sanz L and Glancy S 2010 All-optical generation of states for "Encoding a qubit in an oscillator" *Opt. Lett.* **35** 3261–3
[25] Bouillard M, Boucher G, Ferrer Ortas J, Pointard B and Tualle-Brouri R 2019 Quantum storage of single-photon and two-photon Fock states with an all-optical quantum memory *Phys. Rev. Lett.* **122** 210501
[26] Alibart O, D'Auria V, De Micheli M, Doutre F, Kaiser F, Labonté L, Lunghi T, Picholle E and Tanzilli S 2016 Quantum photonics at telecom wavelengths based on lithium niobate waveguides *J. Opt.* **18** 104001
[27] Wasilewski W, Lvovsky A I, Banaszek K and Radzewicz C 2006 Pulsed squeezed light: simultaneous squeezing of multiple modes *Phys. Rev.* A **73** 063819
[28] Brańczyk A M, Ralph T C, Helwig W and Silberhorn C 2010 Optimized generation of heralded Fock states using parametric down-conversion *New J. Phys.* **12** 063001
[29] Roman-Rodriguez V, Brecht B, Srinivasan K, Silberhorn C, Treps N, Diamanti E and Parigi V 2021 Continuous variable multimode quantum states via symmetric group velocity matching *New J. Phys.* **23** 043012
[30] Flühmann C, Nguyen T L, Marinelli M, Negnevitsky V, Mehta K and Home J P 2019 Encoding a qubit in a trapped-ion mechanical oscillator *Nature* **566** 513–17
[31] Campagne-Ibarcq P *et al* 2020 Quantum error correction of a qubit encoded in grid states of an oscillator *Nature* **584** 368–72
[32] Ourjoumtsev A, Tualle-Brouri R, Laurat J and Grangier P 2006 Generating optical Schrödinger kittens for quantum information processing *Science* **312** 83–86
[33] Ra Y-S, Dufour A, Walschaers M, Jacquard Clement, Michel T, Fabre C and Treps N 2020 Non-Gaussian quantum states of a multimode light field *Nat. Phys.* **16** 144–7
[34] Serino L, Gil-Lopez J, Stefszky M, Ricken R, Eigner C, Brecht B and Silberhorn C 2022 Realization of a multi-output quantum pulse gate for decoding high-dimensional temporal modes of single-photon states (arXiv:2211.05693 [physics, physics: quant-ph])
[35] Fukui K, Takeda S, Endo M, Asavanant W, Yoshikawa J-ichi, van Loock P and Furusawa A 2022 Efficient backcasting search for optical quantum state synthesis *Phys. Rev. Lett.* **128** 240503